

Oligocrystalline Shape Memory Alloys

Stian M. Ueland, Ying Chen, and Christopher A. Schuh*

Copper-based shape memory alloys (SMAs) exhibit excellent shape memory properties in single crystalline form. However, when they are polycrystalline, their shape memory properties are severely compromised by brittle fracture arising from transformation strain incompatibility at grain boundaries and triple junctions. Oligocrystalline shape memory alloys (oSMAs) are microstructurally designed SMA structures in which the total surface area exceeds the total grain boundary area, and triple junctions can even be completely absent. Here it is shown how an oligocrystalline structure provides a means of achieving single crystal-like SMA properties without being limited by constraints of single crystal processing. Additionally, the formation of oSMAs typically involves the reduction of the size scale of specimens, and sample size effects begin to emerge. Recent findings on a size effect on the martensitic transformation in oSMAs are compared and a new regime of heat transfer associated with the transformation heat evolution in these alloys is discussed. New results on unassisted two-way shape memory and the effect of loading rate in oSMAs are also reported.

1. Introduction

Oligocrystalline shape memory alloys (oSMAs) are shape memory alloys (SMAs) in which the total surface area is greater than the total grain boundary area. This inflated proportion of surface area allows the martensitic phase transformation, which is the physical mechanism underlying the shape memory effect, to proceed in a much less constrained environment than in a conventional polycrystal. As a result, whereas the introduction of a conventional polycrystalline structure to Cu-based SMAs severely compromises the excellent single crystal properties to a point where they are considered inadequate for commercial application, oSMAs have a unique grain architecture that does not suffer the same drawbacks. Because grains in oSMAs are mostly surrounded by unconfined free surfaces rather than other grains, oSMA structures are capable of achieving single crystal-like properties, but with much less stringent processing restrictions on material volume and shape and also at much lower processing cost.

S. M. Ueland, Prof. Y. Chen,^[+] Prof. C. A. Schuh
Department of Materials Science and Engineering
Massachusetts Institute of Technology
77 Massachusetts Avenue, Cambridge, MA 02139, USA
E-mail: schuh@mit.edu

[+] Present address: Department of Materials Science
and Engineering, Rensselaer Polytechnic Institute,
110 8th Street, Troy, NY 12180, USA



DOI: 10.1002/adfm.201103019

The combination of single crystal-like properties as well as scalable and cost-effective processing offered by oSMAs is therefore particularly attractive for the development of new, commercially competitive SMA structures. Recently significant effort has been devoted to demonstrate their experimental viability. So far, oSMA wires and foams have been developed, and they all exhibit superior performance compared to their bulk polycrystalline counterparts.^[1–6] For example, Chen et al. showed completely recoverable strains up to about 7% in Cu-Al-Ni oSMA wires which normally fracture at very small strains.^[1] Subsequently, fatigue properties were studied in Cu-Zn-Al oSMA wires, which showed a dramatic increase in the number of cycles to failure of up to two orders of magnitude over conventional polycrystals.^[3] In these cases, microstructural design has rendered otherwise brittle

SMA materials both flexible and resistant to fracture.

The purpose of this paper is twofold. First, it serves as a brief review of our work on the processing, characterization, and properties of oSMAs, with emphasis on some novel physical phenomena that have been discovered in this new class of smart materials. Second, throughout this paper we introduce new results on the key properties of both Cu-Al-Ni and Cu-Zn-Al oSMAs; these results particularly highlight some of the key unresolved issues, as well as the interesting opportunities, for the development and optimization of oSMAs for applications as a new class of smart materials.

2. Superelasticity and Shape Memory

Because of their low raw materials cost, Cu-based shape memory alloys have long been considered a commercially attractive alternative to the more expensive Ni-Ti alloys. In the form of single crystals, their properties are excellent, as exemplified by the large reversible superelastic strain they can achieve; an example is shown in **Figure 1d**, obtained in Cu-Al-Ni by Otsuka et al.^[7] In polycrystals, on the other hand, stress concentrations near grain boundaries and triple junctions during martensitic transformations frequently lead to early fracture. An example of this from the work of Sakamoto et al. is shown in **Figure 1a**.^[8] Because of the very high processing costs associated with single crystal production and the brittleness of polycrystalline materials, this class of SMAs is generally excluded from consideration for most SMA applications.

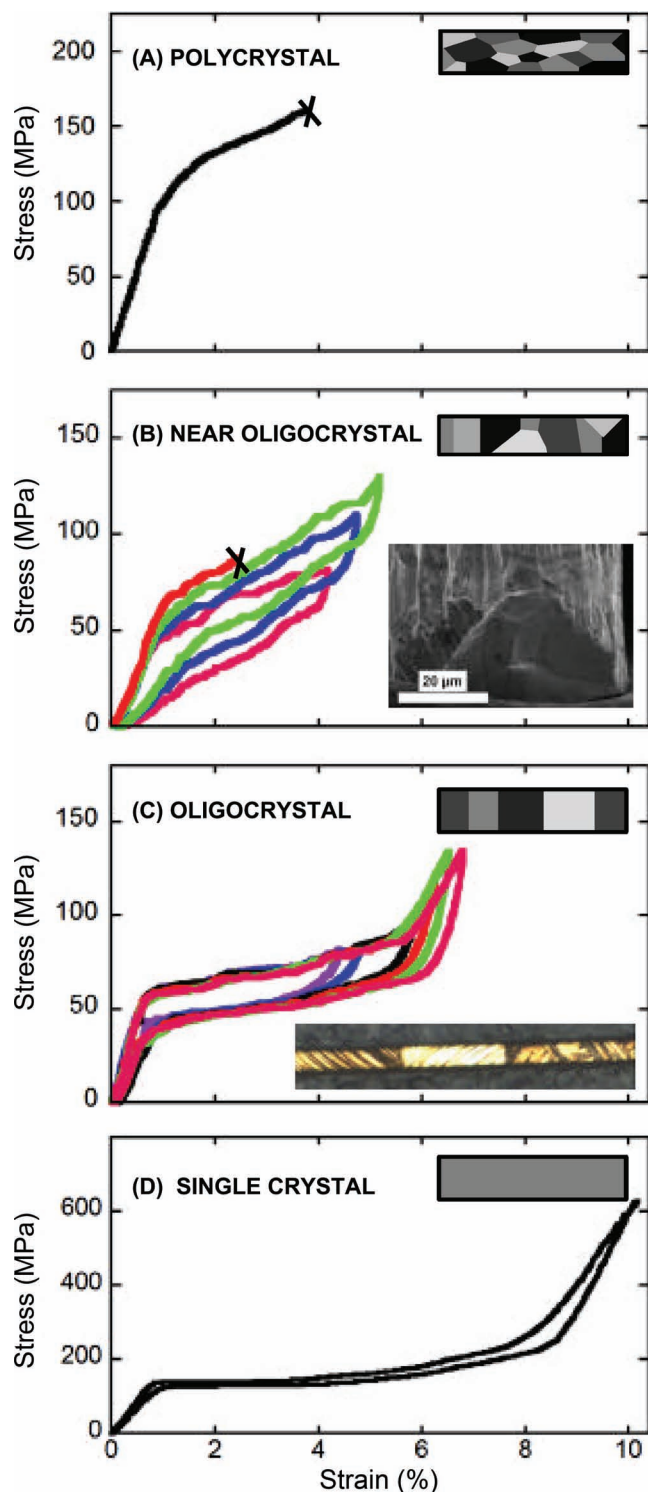


Figure 1. Stress-strain curves of a) polycrystalline Cu-14.1Al-4.2Ni,^[8] b) near oligocrystalline Cu-13.7Al-5Ni containing a triple junction (see inset), c) oligocrystalline Cu-13.7Al-5Ni, and d) single crystalline Cu-14Al-4Ni.^[7] The schematics in the top right corner of each graph show the grain structure of each sample.

oSMA structures were developed to overcome these limitations and to reproduce the desirable SMA properties of single crystals without incurring their high processing cost. Figure 1c

shows an example of an oligocrystalline Cu-Al-Ni wire undergoing several consecutive superelastic cycles without failure.^[1] The inset shows the bamboo structure of such an oSMA wire, where grains span the entire wire cross-section and grain boundaries are generally perpendicular to the wire axis. The superelastic characteristics of the oligocrystal lie between those of the single crystal and the polycrystal, but approach more closely those of the single crystal. In oSMAs, because grain boundaries are sparse and triple junctions are absent, there are very few places where transformation strain must be accommodated. Furthermore, because of surface relaxation, the stresses at existing grain boundaries are considerably reduced. Each individual grain is therefore largely unconstrained and free to undergo the transformation as if it were a single crystal. The single crystal-like superelasticity of oSMA structures is not limited to just a single superelastic cycle, but instead persists over many subsequent cycles. Ueland and Schuh reported that Cu-Zn-Al oSMA wires exhibited fatigue life that is almost two orders of magnitude longer than for conventional polycrystalline SMAs of the same alloy, and approaching those of single crystals.^[3]

However, oligocrystalline wires do not necessarily always have perfect bamboo grain structures and can be compromised by the occasional presence of triple junctions. This is illustrated in Figure 1b, where the stress-strain curves of a Cu-Al-Ni microwire with an imperfect bamboo structure are plotted. Unlike a bulk polycrystal, this wire exhibited some degree of reversible superelasticity. However, it fractured during the fourth cycle. Investigation after failure revealed a brittle intergranular fracture with clear evidence of a triple junction at the fracture surface (see inset). Thus, the presence of a single triple junction can potentially compromise the fatigue properties of an oSMA in some cases. This clearly has significant implications for the engineering scale-up of long wires, foams, or other potential oligocrystalline structures and calls for thorough study of weak-link physics in oSMAs.

In addition to superelastic properties (where the wires were tested at a constant temperature above the austenite finish temperature A_f) as discussed above, the complementary property of stress-assisted two-way shape memory has also been confirmed to exist in oSMAs.^[1–3] In those tests, the oSMAs are subject to thermal cycling under an applied constant stress, which favors the formation of some specific martensite variants over others, and this in turn biases the material shape under stress (i.e., biases the length for the present case of wires). For some practical purposes, however, the stress-free two-way memory effect, whereby no external stress is needed to bias the preferred shape of the material, is desired. This property usually requires a number of prior training steps (e.g., superelastic cycling above A_f), which, in light of the improved fatigue life of oSMAs, can easily be performed.^[3,9] The purpose of training is to develop a microstructural asymmetry in the austenite matrix that assists the nucleation and growth of a preferred martensite plate arrangement during cooling.^[9,10]

We report here that in at least one family of oSMAs, unassisted shape memory can be achieved by using superelastic cycling as a means of training. A Cu-22.9Zn-6.3Al (wt%) wire with a diameter of 114 μm , gauge length of 4.5 mm, and austenite finish temperature, $A_f = 35^\circ\text{C}$, was used in this experiment; further details on the processing and properties of

this material can be found elsewhere.^[3] The unassisted two-way shape memory effect is revealed by a thermal cycle between -5°C and 40°C at the rate of $1^{\circ}\text{C min}^{-1}$ under a constant tensile load of 0.1 MPa ; here such a small tensile load is applied to enable the measurement of transformation strain and the small load itself should only have trivial if not entirely negligible effect on the transformations. The training for the wire is mechanical cycling between the unloaded state and 55 MPa (resulting in $\approx 4.2\%$ strain) isothermally at 40°C . The wire was initially heated to 40°C , and then was subjected to one thermal cycle followed by a mechanical cycle, and subsequently another thermal cycle. Afterwards continuous mechanical cycling at 40°C was performed, interrupted by a thermal cycle after 3, 6, 16, and 40 mechanical cycles. The strain-temperature plot of the first thermal cycle (before training) as well as the thermal cycle after 40 mechanical training cycles are shown in Figure 2a. The recoverable strain has increased from $\approx 1.2\%$ prior to training to $\approx 3.2\%$ after training. Figure 2b shows the

evolution of the two-way memory strain as the wire is subjected to succeeding training steps as well as the evolution of the characteristic energy dissipation per unit strain of the mechanical cycles (training cycles). The two-way memory effect and the mechanical hysteresis size evolve in a similar manner and both of them stabilize rather quickly; there is a dramatic increase/decrease during the first few cycles followed by a much more subtle variation.

In single crystal Cu-Zn-Al, the two-way shape memory strain can be large, but it normally requires a large number of training cycles.^[11–13] For polycrystals of the same alloy family, the development of reproducible microstructure characteristics during training is faster, i.e., it requires only a few training cycles, similar to the case of the oSMA shown in Figure 2, but the attainable shape memory strain is generally only slightly higher than 1% .^[9,14] Grain boundaries in polycrystals, which can be preferential martensite nucleation sites, might facilitate the formation of certain martensite configurations, but in the meantime they also impose constraints on the extent of the transformation and thus limit the maximum unassisted shape memory strain attainable. Compared with single crystals and polycrystals, oligocrystalline SMAs may therefore potentially be the optimal microstructure for unassisted shape memory. They contain a reasonable number of grain boundaries to promote the prompt formation of preferred martensite configuration, but the total grain boundary area is very small compared to the unconstrained surface area and therefore a large recoverable strain close to those in single crystals can be attained in them.

3. Size Effects

The development of the oSMA structure generally involves the reduction of one or more sample dimensions, normally to below the millimeter range. Interestingly, the diameters of oSMA microwires reported in our prior and present work ($\approx 20\text{--}100\text{ }\mu\text{m}$) constitute a range of characteristic length scales largely unexplored in prior work on SMAs.^[1–3] The development of oSMAs has therefore enabled systematic exploration of sample size effects upon the martensitic phase transformation. For both Cu-Al-Ni and Cu-Zn-Al it was found that smaller wires exhibit larger hysteresis than larger ones, i.e., smaller wires dissipate more energy in a superelastic cycle than larger wires.^[2,3] The various possible origins for the size effect were analyzed by Chen and Schuh, who concluded that free surfaces enhanced the internal frictional work associated with propagating martensite/austenite phase boundaries.^[2]

In Figure 3 we assemble all available experimental data which together speak to this issue. Here the stress hysteresis $\Delta\sigma$ is plotted against the sample diameter, D , for our microwires (red data points for Cu-Zn-Al and blue for Cu-Al-Ni), in addition to literature results for millimeter-scale single crystal specimens of the same alloys, a bamboo structured Cu-Mn-Al wire with $D = 1\text{ mm}$, and single crystalline micro- and nanopillars.^[7,15–19] There is a very good agreement between the data for the two oSMAs that have been studied systematically over the range $D \approx 20\text{--}100\text{ }\mu\text{m}$; for both of these the hysteresis increases as the wire diameter decreases. A power-law fit of the type $\Delta\sigma \propto D^a$ yields a scaling exponent of -0.66 for these data.

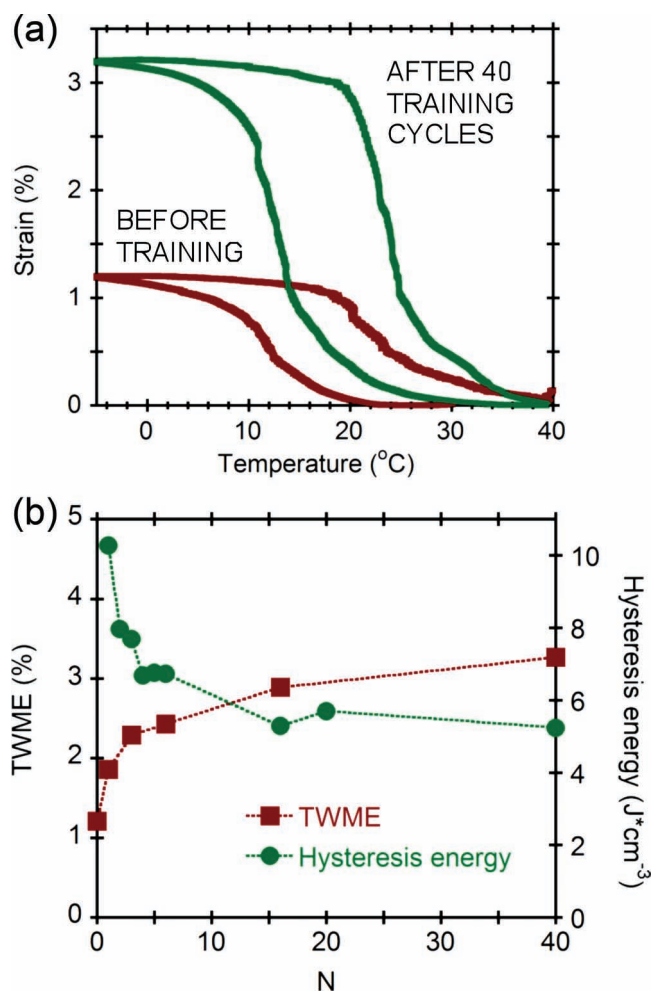


Figure 2. a) Stress free two-way shape memory effect before and after training. b) Evolution of the two-way memory effect (TWME) with the number of training cycles (squares) and evolution of the hysteresis energy per superelastic cycle with the number of mechanical cycles (circles). The hysteresis energy is the energy dissipated in a superelastic cycle normalized by the strain amplitude.^[2]

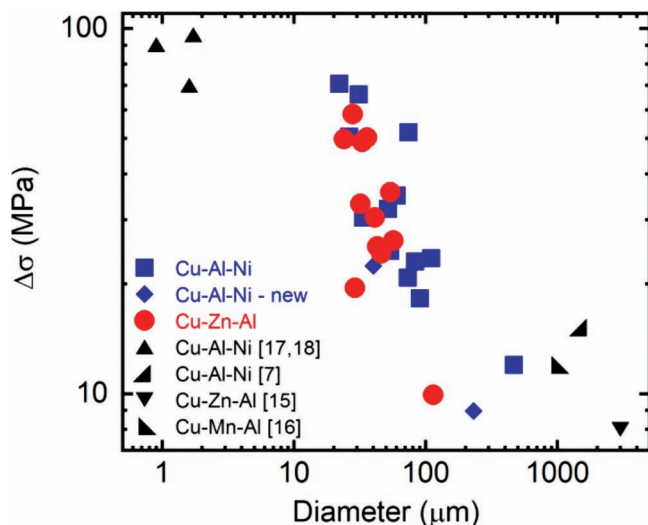


Figure 3. Dependence of the stress hysteresis $\Delta\sigma$ on sample diameter D . The data for Cu-Al-Ni microwires are from ref. [2], except for the two points marked as new; Cu-Zn-Al microwires are from ref. [3] and data for the first cycle are used. Data for nanopillars are extracted from ref. [17,18] and data points from large millimeter-scale samples are from ref. [7,15,16].

In addition, these data on oSMAs smoothly connect to the data for single crystals larger than 100 μm , above which the wire diameter no longer apparently affects the hysteresis size. They are also reasonably consistent with the data for single crystalline micro- and nanopillars of Cu-Al-Ni with diameters around 1 μm , which also exhibit a large hysteresis.

4. Heat Transfer and Rate Effects

The first-order phase transformations in SMAs involve the release and absorption of latent heat during the forward and reverse transformations, respectively. As a result, heat transfer has long been known to play a critical role in the superelastic properties of SMAs. However, the introduction of small-scale samples of oSMA has brought to light a new regime in which heat transfer has a different effect.

The “classical” heat transfer situation in SMAs, which leads to a classical size effect on their hysteresis, is present in conventional “bulk” samples with dimensions above about 1 mm. In such samples, heat transfer is limited by convection. The slow exchange of heat between the sample and the environment results in temperature changes within the sample and thus the test is no longer truly isothermal. Because the phase transformations underlying SMA properties are temperature dependent, the temperature change directly affects the measured mechanical hysteresis. The effect of heat accumulation during superelastic loading in conventional SMAs can be most easily revealed by testing them at different strain rates: at slow rates the samples remain in thermal equilibrium with the environment, while at faster rates the heat is generated or absorbed at a faster pace than it is exchanged. For example, Otsuka et al. found a strong positive correlation between the hysteresis size and the strain rate for strain rates between 1.7×10^{-5} and

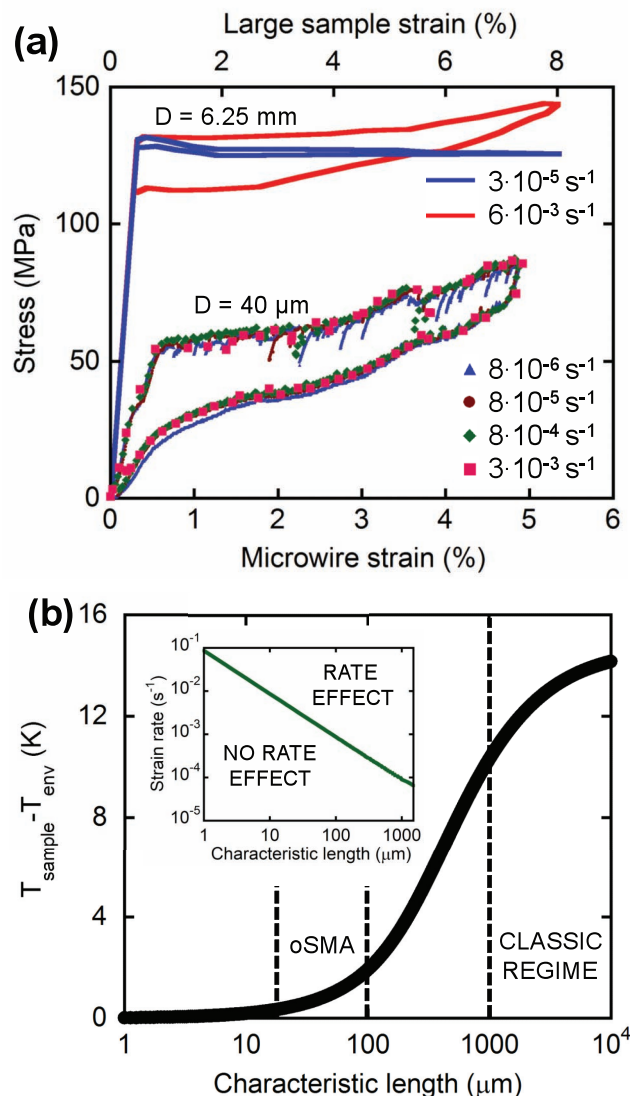


Figure 4. a) Successive stress–strain curves at four strain rates for a Cu-Al-Ni wire with a diameter of 40 μm tested at 60 $^{\circ}\text{C}$, compared to two stress–strain curves at comparable strain rates of a single crystalline Cu-Zn-Al rod with a diameter of 6.25 mm from ref. [22]. b) Temperature evolution versus sample characteristic length for a strain rate of $8 \times 10^{-4} \text{ s}^{-1}$. The inset shows a line corresponding to a temperature increase of 2 K during the forward transformation in the strain rate–length scale space; this line serves as a threshold above which rate effect is expected to emerge.

$1.7 \times 10^{-2} \text{ s}^{-1}$ in Cu-Al-Ni.^[7] Similarly, rate has been observed to affect hysteresis shape and size in Ni-Ti with rates varying between 2.8×10^{-4} – $2.5 \times 10^{-1} \text{ s}^{-1}$, as well as in Cu-Al-Be for two rates of 2.3×10^{-5} and $1.4 \times 10^{-2} \text{ s}^{-1}$.^[20,21]

In Figure 4a we have adapted two typical stress–strain curves for a single crystalline Cu-Zn-Al rod with a diameter of 6.25 mm tested at room temperature at $3 \times 10^{-5} \text{ s}^{-1}$ and $6 \times 10^{-3} \text{ s}^{-1}$; the strain rate effect is evident in this large sample and the average hysteresis at the fast rate is about eight times that obtained at the slower rate.^[22]

Here we report for the first time results from testing oSMA wires at various strain rates spanning almost three orders of magnitude. Figure 4a shows superelastic loops of a Cu-14Al-4Ni (wt%) oSMA wire of 40 μm diameter and a gauge length of 2.2 mm, tested at 60 $^{\circ}\text{C}$. The wire was tested at four different strain rates, over a range where strain rate effects have been observed in conventional bulk SMAs.^[20,21] Interestingly, stress relaxation during martensitic transformation at slow strain rates, such as at $8 \times 10^{-6} \text{ s}^{-1}$ and at $8 \times 10^{-5} \text{ s}^{-1}$, can be easily seen on the loading curve, and this has not been (and cannot be) observed in prior tests performed at constant force ramping rates.^[1–3] The observed stress relaxation reflects the heterogeneous or jerky nature (both spatially and temporally) of martensitic transformation and the large extent of relaxation that can occur in such oSMAs at small scales.

However, despite the presence of relaxation at slow rates and the difference in the extent of relaxation at different rates, the four superelastic cycles for the oSMA wires shown in Figure 4a at these dramatically different rates almost completely overlap each other. This suggests that within the explored rate range, strain rate does not affect the measured mechanical hysteresis in such oSMA wires and that heat convection is likely not the limiting mechanism in these small structures. The classical rate effect caused by sluggish heat convection in large SMAs does not come into play at small length scales (below $\approx 100 \mu\text{m}$) because heat is effectively exchanged by virtue of the large surface area.

Chen and Schuh, in their discussion on physical origins of the size effects seen in oSMA Cu-Al-Ni, suggested that these structures, with characteristic dimensions below $\approx 100 \mu\text{m}$, occupy a unique regime for heat transfer considerations.^[2] They estimated the temperature evolution in wires as

$$T_{\text{sample}}(t) = T_{\text{env}} + \frac{Q_{\text{tot}}}{\rho C_p} \frac{\tau}{t_0} \left[1 - \exp\left(-\frac{t}{\tau}\right) \right] \quad (1)$$

with T_{env} the ambient temperature, Q_{tot} the total heat released, ρ the density, C_p the specific heat capacity, τ the thermal time constant incorporating a convection coefficient, and t_0 the time span of the transformation. Using $t_0 = 60 \text{ s}$ (corresponding to a strain rate of $8 \times 10^{-4} \text{ s}^{-1}$ for a total strain of 5%), $Q_{\text{tot}} = 4.62 \times 10^7 \text{ J m}^{-3}$, $\rho = 7140 \text{ kg m}^{-3}$, and $C_p = 440 \text{ J (kg K)}^{-1}$, the temperature increase of a Cu-Zn-Al SMA at the end of forward transformation (i.e., $t = t_0$) is calculated as a function of the characteristic length scale (which is incorporated into the thermal constant τ and is proportional to τ) and plotted in Figure 4b. As the graph shows, Equation (1) predicts a large temperature rise of about 14 K for large samples with a characteristic length above roughly 1 mm. For oligocrystalline wires, on the other hand, the temperature increase is small; it is at most 2 K for wires with diameters around 100 μm and is nearly negligible when the size is reduced to 20 μm .

We also show in the inset of Figure 4b the partition of the strain rate-length scale space into the rate-dependent regime and rate-independent regime as far as the heat transfer effect is concerned. The green line that separates the two regimes is determined by solving for t_0 in Equation (1) at different characteristic lengths while setting the allowed increase in sample temperature to be 2 K and the total strain to 5%. In the upper

right regime, which corresponds to large length scales and high strain rates, the temperature change can be rather significant and rate effects are therefore expected to occur. In the lower left regime of small length scales and low strain rates, heat convection is extremely rapid and thus temperature change is predicted to be sufficiently small that rate effects can be neglected. Therefore the classical rate effects known in SMAs should not apply to oSMA wires with fine diameters.

On a side note, the classical rate effects resulting from temperature variations are also not expected to be relevant in micromachined single crystalline SMA pillars with diameters around or below only 1 μm , but for a different reason.^[18] As these pillars are only a few micrometers in height and are attached to the substrate SMA (they are essentially one piece of material), heat conduction between the pillar and the substrate is extremely fast as compared to the convection of heat from the pillar to the environment. Therefore heat conduction is the major heat transfer mechanism by which heat is released or absorbed in the pillar, and this would be sufficiently rapid that the temperature in the pillar remains constant. In summary, for both the present oSMA microwires and the micro- or nanopillars, the reported significant increase in mechanical hysteresis is not related to temperature variations.

The present data on strain rate independence of the mechanical hysteresis also have significant implications for the physical origins of the hysteresis itself and the true cause for the observed size effect in hysteresis shown in Figure 3, now that heat transfer has been ruled out as a primary cause in small oSMA structures. As the mechanical energy corresponding to the area within the hysteresis loop is essentially lost to the environment as heat, the increase in hysteresis in small oSMA structures must result from an increase in the generated heat during isothermal transformations. In line with the suggestion of Chen and Schuh, this points to a possible mechanism of enhanced internal frictional work in oSMA structures.^[2] Interestingly, internal frictional work has long been recognized to eventually be dissipated as heat and bear little or no rate dependence.^[23,24]

5. Conclusions

In summary, we have reviewed recent studies on oligocrystalline shape memory alloys (oSMAs) and compared their performance to conventional single crystal and polycrystalline SMAs; we have also introduced a variety of new experimental observations, e.g., unassisted shape memory, to highlight the interesting and unusual properties of this new class of smart materials. The formation of an oligocrystalline structure constitutes a means of overcoming the brittleness of Cu-based polycrystalline SMAs and achieving single crystal-like properties, without incurring the cost and constraints of single crystal processing. The reduced dimensions of oSMA wires also give rise to interesting and potentially useful new phenomena, such as a mechanical hysteresis that increases as the sample size is reduced. The small size of many oSMAs also allows for rapid heat exchange with their surroundings during martensitic transformations. As a result, classical strain rate effects associated with sluggish heat transfer in SMAs do not apply to small oSMAs and we demonstrate rate independence in those materials here.

Acknowledgements

This work was supported by the US Office of Army Research, through the Institute for Soldier Nanotechnologies at MIT.

Received: December 13, 2011

Published online: March 1, 2012

-
- [1] Y. Chen, X. X. Zhang, D. C. Dunand, C. A. Schuh, *Appl. Phys. Lett.* **2009**, 95, 171906.
- [2] Y. Chen, C. A. Schuh, *Acta Mater.* **2011**, 59, 537.
- [3] S. M. Ueland, C. A. Schuh, *Acta Mater.* **2012**, 60, 282.
- [4] M. Chmielus, X. X. Zhang, C. Witherspoon, D. C. Dunand, P. Mullner, *Nat. Mater.* **2009**, 8, 863.
- [5] G. Bertolino, A. Gruttadauria, P. A. Larochette, E. M. Castrodeza, A. Baruj, H. E. Troiani, *Intermetallics* **2011**, 19, 577.
- [6] D. C. Dunand, P. Mullner, *Adv. Mater.* **2011**, 23, 216.
- [7] K. Otsuka, C. M. Wayman, K. Nakai, H. Sakamoto, K. Shimizu, *Acta Metall. Mater.* **1976**, 24, 207.
- [8] H. Sakamoto, Y. Kijima, K. Shimizu, *Trans. Jpn. Inst. Met.* **1982**, 23, 585.
- [9] R. Stalmans, J. Van Humbeeck, L. Delaey, *Acta Metall. Mater.* **1992**, 40, 501.
- [10] J. Perkins, R. O. Sponholz, *Metall. Trans. A* **1984**, 15, 313.
- [11] J. Malarria, F. C. Lovey, M. Sade, *Mater. Sci. Eng., A* **2009**, 517, 118.
- [12] C. Picornell, M. Sade, E. Cesari, *Metall. Mater. Trans. A* **1994**, 25, 687.
- [13] J. Pons, M. Sade, F. C. Lovey, E. Cesari, *Mater. Trans. JIM* **1993**, 34, 888.
- [14] P. A. Larochette, M. Ahlers, *Mater. Sci. Eng., A* **2003**, 361, 249.
- [15] E. Vives, S. Burrows, R. S. Edwards, S. Dixon, L. Manosa, A. Planes, R. Romero, *Appl. Phys. Lett.* **2011**, 98, 011902.
- [16] Y. Sutou, T. Omori, K. Yamauchi, N. Ono, R. Kainuma, K. Ishida, *Acta Mater.* **2005**, 53, 4121.
- [17] J. S. Juan, M. L. No, C. A. Schuh, *Nat. Nanotechnol.* **2009**, 4, 415.
- [18] J. S. Juan, M. L. No, C. A. Schuh, *J. Mater. Res.* **2011**, 26, 2461.
- [19] J. S. Juan, M. L. No, C. A. Schuh, *Adv. Mater.* **2008**, 20, 272.
- [20] G. N. Dayananda, M. S. Rao, *Mater. Sci. Eng., A* **2008**, 486, 96.
- [21] D. Entemeyer, E. Patoor, A. Eberhardt, M. Berveiller, *Int. J. Plasticity* **2000**, 16, 1269.
- [22] J. Van Humbeeck, L. Delaey, *J. Phys. (Paris)* **1981**, 42, 1007.
- [23] J. Ortin, A. Planes, *Acta Metall. Mater.* **1988**, 36, 1873.
- [24] P. Wollants, J. R. Roos, L. Delaey, *Prog. Mater. Sci.* **1993**, 37, 227.
-